ORIGINAL PAPER

CrossMark

S100P and Ezrin promote trans-endothelial migration of triple negative breast cancer cells

Kyoko Kikuchi[1] · Keely May McNamara[1] · Yasuhiro Miki[2] · Erina Iwabuchi[1] · Ayako Kanai[1,3] · Minoru Miyashita[3] · Takanori Ishida[3] · Hironobu Sasano[1]

Abstract

Purpose Triple negative breast cancer (TNBC) patients generally have an adverse clinical outcome because their tumors often recur and metastasize to distant sites in the first 3 years after surgery. Therefore, it has become pivotal to identify potential factors associated with metastasis. Here, we focused on the effects of S100P and Ezrin on the trans-endothelial migration (TEM) of TNBC cells, as they have both been suggested to play a role in this process in other malignancies.

Methods The expression of S100P and Ezrin was examined by immunohistochemistry in 58 primary TNBC samples. The mRNA and protein levels of S100P and Ezrin were assessed in breast cancer-derived cell lines using qRT-PCR and Western blotting, respectively. Proliferation and migration assays were performed using TNBC-derived MFM-223 and SUM-185-PE cells transfected with S100P and Ezrin siRNAs. Two different timeframes were employed for TEM assays using TNBC-derived cells and human umbilical vein endothelial-derived cells, respectively. Correlations between the status of Ezrin$^{Thr-567}$ expression and various clinicopathological features were analyzed by immunohistochemistry.

Results We found that S100P and Ezrin double negative TNBC cases were significantly associated with a better disease-free survival. We also found that single and double siRNA-mediated knockdown of S100P and Ezrin in TNBC-derived cells significantly inhibited their TEM and destabilized the intercellular junctions of endothelial cells. In addition, we found that Ezrin$^{Thr-567}$ immunoreactivity significantly correlated with vascular invasion in TNBC patients.

Conclusions From our data we conclude that S100P, Ezrin and Ezrin$^{Thr-567}$ are involved in the trans-endothelial migration of TNBC cells and that they may serve as potential targets in TNBC patients.

Keywords Triple negative breast carcinoma · S100P · Ezrin · Trans-endothelial migration

✉ Hironobu Sasano
hsasano@patholo2.med.tohoku.ac.jp

1   Department of Pathology, Tohoku University Graduate School of Medicine, 2-1, Seiryo-machi, Aoba-ku Sendai-shi, Miyagi 980-8575, Japan

2   Department of Disaster Obstetrics and Gynecology, International Research Institute of Disaster Science (IRIDeS), Tohoku University, 2-1, Seiryo-machi, Aoba-ku Sendai-shi, Miyagi 980-8575, Japan

3   Department of Breast and Endocrine Surgical Oncology, Tohoku University Graduate School of Medicine, 2-1, Seiryo-machi, Aoba-ku Sendai-shi, Miyagi 980-8575, Japan

1 Introduction

Triple negative breast cancer (TNBC) is defined by absence of the estrogen receptor, progesterone receptor and human epidermal growth factor receptor 2 (HER2). Treatment of TNBC patients has been challenging due to the intratumoral heterogeneity and the lack of specific targeted therapies [1]. The only systemic treatment option available is chemotherapy with standard cytotoxic agents including anthracyclines and taxane combination treatment [2, 3]. TNBC patients have generally an adverse clinical outcome due to recurrences and metastases to distant organs such as bone, lung brain and liver in the first 3 years following the first surgery [4–7]. Therefore, it is pivotal to identify factors that can predict postoperative metastasis at the time of surgery.

S100P is a member of the S100 family of small calcium-binding proteins containing an EF hand motif that has a

high affinity for calcium. S100P has been found to have multiple functions, including calcium homeostasis, differentiation and proliferation regulation [8–12]. It was first detected in placenta and later in various other normal tissues [13]. S100P has also been found to be expressed in diverse malignancies, and to be associated with their proliferation, metastasis and poor clinical outcome [8, 14]. Although S100P expression has also been found to be elevated in TNBC tissues [15] and to be associated with a poor survival of TNBC patients [16], its exact role and mode of action still remain to be established.

Ezrin is a member of the ERM (Ezrin, Radixin, Moesin) family of proteins that links F-actin to the cell membrane following phosphorylation, thereby playing an important role in structure formation of cells, motility and endocytosis [17, 18]. The C-terminal domain of ERM proteins is capable of binding to the N-terminal domain of the same molecule, resulting in a dormant conformation [19]. ERM proteins are activated after binding of the N-terminal domain to PIP2 (Phosphatidylinositol 4, 5-bisphosphate), which is located at the cell membrane, after which threonine residues are phosphorylated (i.e., Ezrin T567, Radixin T564, Moesin T558) [19–21]. Ezrin has been reported to be upregulated in various cancer tissues compared to their normal counterparts, including breast and lung cancer, and has been associated with tumor invasion and metastasis [22–25]. However, the mechanisms underlying the role of Ezrin in these processes have so far remained unknown.

It has been suggested that S100P dimers, formed in response to increases in cellular calcium concentrations, can bind and activate Ezrin [26–28]. This interaction has been reported to promote trans-endothelial migration (TEM) in lung and pancreatic cancer patients [29–31]. As yet, the effect of this interaction in breast cancer patients, particularly TNBC patients, has not been examined. Here, we set out to elicit possible effects of S100P and Ezrin on the TEM of TNBC cells.

2 Materials and methods

2.1 Patients

In total 58 paraffin-embedded TNBC tissue specimens were obtained from patients undergoing surgical resection from 1998 to 2008 at Tohoku University Hospital (Miyagi, Japan) for immunohistochemistry. The mean age of the patients was 55.3 years (range: 30 to 81 years). This study was approved by the Ethics Committee at the Tohoku University School of Medicine (2012–1-185). Informed consent was obtained from all patients.

2.2 Immunohistochemistry

A Histofine kit (Nichirei Bioscience, Tokyo, Japan), based on a biotin-streptavidin method, was used for immunohistochemistry (IHC). Paraffin sections (3 μm thick) were dewaxed with xylene and ethanol. Next, antigen retrieval was performed by heating the slides in an autoclave at 121 °C for 5 min in antigen retrieval buffer, pH 9.0 (Nichirei Bioscience) for S100P immunostaining, and in a microwave for 20 min in citrate buffer, pH 6.0 for Ezrin and Ezrin$^{Thr-567}$ immunostaining. The sections were subsequently washed with PBS and incubated for 30 min at room temperature with blocking solution, after which they were incubated overnight at 4 °C with primary antibodies. The conditions of the primary antibodies employed in this study are listed in Table 1. Endogenous peroxidase activity was quenched by immersing the slides in 0.3% hydrogen peroxide in methanol for 30 min at room temperature. The sections were subsequently incubated with a biotinylated secondary antibody for 30 min at room temperature and peroxidase labeled using a streptavidin solution. Finally, the proteins were visualized using a 3, 3-diaminobenzidine (DAB) solution and the sections were counterstained with hematoxylin. Normal stomach, colon and skin were used as positive controls for S100P, Ezrin and Ezrin$^{Thr-567}$ staining, respectively. In order to evaluate cytoplasmic expression of the proteins, a semi-quantitative scale (Immunoreactive

Table 1 Antibodies used in this study

Antigen	Clone	Species	Reference	Dilution		
				IHC	WB	ICC
S100P	EPR6143	Rabbit	Abcam	1:500	1:200	
Ezrin	Polyclonal	Rabbit	CST	1:100	1:1000	
Ezrin$^{Thr-567}$	Polyclonal	Rabbit	SAB	1:1000		
β-actin	AC-15	Mouse	Sigma		1:1000	
Pan-cytokeratin	AE1/AE3	Mouse	Abcam			1:200

CST, Cell Signaling Technologies (Danvers, MA, USA); *SAB*, Signalway Antibody (College Park, MD, USA); *Sigma*, Sigma-Aldrich (St. Louis, MO, USA); *IHC*, Immunohistochemistry; *WB*, Western blotting; *ICC*, Immunocytochemistry

Table 2 Primer sequences used in this study

Target	Sequence (5′ → 3′)	
RPL13A	Forward	GAT CCA CTA CCG GAA GAA ACA G
	Reverse	ATG GAG GAA GGG CAG GCA AC
S100P	Forward	ACG CAG ACC CTG ACC AA
	Reverse	ACG AAC ACG ATG AAC TCA CTG
Ezrin	Forward	CGC TCT AAG GTT CTG CTC T
	Reverse	TCC TGG GCA GAC ACC TTC TTA
CDH1 (E-cadherin)	Forward	GCC TCC TGA AAA GAG AGT GGA AG
	Reverse	TGG CAG TGT CTC TCC AAA TCC G
Vimentin	Forward	TCA GAA TAT GAA GGA GGA AAT GGC
	Reverse	GAG TGG GTA TCA ACC AGA GGG AGT

Score (IRS)) was applied, which takes into account the intensity of the color reaction (0: no reaction, 1: weak reaction, 2: moderate reaction, 3: intense reaction) as well as the proportion of positive cells (0: no positive cells, 1: < 10% positive cells, 2: 10–50% positive cells, 3: 51–80% positive cells, 4: > 80% positive cells) as previously described [12]. The final scores represent the products of points given for the individual characteristics and ranges between 0 and 12. The scores were classified into two groups as follows: low: 0–6, high: 8–12 for S100P, low: 0–4, high: 4–12 for Ezrin and Ezrin[Thr-567].

2.3 Cell culture

The human breast cancer-derived cell lines MCF-7, T-47D, ZR-75-1, SK-BR-3, MDA-MB-231 and MDA-MB-453 were obtained from the American Type Culture Collection (ATCC, Manassas, VA, USA). MCF-7, T-47D, ZR-75-1 and SK-BR-3 cells were cultured in RPMI-1640 medium (Sigma-Aldrich, St. Louis, MO, USA) containing 10% fetal bovine serum (FBS, Biosera, Boussens, France) at 37 °C in an atmosphere containing 5% CO_2. MDA-MB-231 and MDA-MB-453 cells were cultured in Leibovitz's L-15 medium (Life Technologies, Carlsbad, CA, USA) containing 10% FBS at 37 °C in a humidified atmosphere according to the supplier's description. The TNBC-derived cell lines MFM-223 and SUM-185-PE were obtained from the Cell Bank Australia (Westmead, NSW, Australia) and Asterand (Detroit, MI, USA), respectively. MFM-223 cells were cultured in Minimum Essential Medium (Life technologies) containing 10% at 37 °C, 5% CO_2 and SUM-185-PE cells were cultured in HAM F-12 medium (Sigma-Aldrich) containing 5% FBS, 1 μg/ml Hydrocortisone (MP Biomedicals, Santa Ana, CA, USA), 5 μg/ml insulin (Sigma- Aldrich) and 2 mM L-glutamine (Life Technologies) at 37 °C, 5% CO_2. The immortalized human umbilical vein endothelial cell line HUEhT-1 was obtained from the JCRB Cell Bank (Osaka, Japan) and cultured in MCDB131 medium (Thermo Fisher Scientific, Waltham, MA, USA) containing 10% FBS, 0.03 g/L endothelial cell growth supplement (Sigma-Aldrich), 5 μg/ml heparin (Sigma-Aldrich) and 10 mM L-glutamine (Wako: Wako pure chemical industries, Osaka, Japan) at 37 °C, 5% CO_2. Trypsin-EDTA (Life technologies) was used for cell passage.

2.4 Quantitative real-time PCR (qRT-PCR)

Total RNA was extracted using TRI reagent (Cosmo Bio, Tokyo, Japan). After extraction, chloroform (Wako) was added to each sample, followed by shaking, incubation for 3 min at room temperature and centrifugation (13,000 rpm, 4 °C, 15 min). The resulting water phase was transferred to clean

Table 3 Target sequences used in this study

Targets	Sequence (5′ → 3′)		Concentration
S100P #1	Sense	CCU GUC ACA AGU ACU UUG AGA TT	5 nM
	Anti-sense	UCU CAA AGU ACU UGU GAC AGG TT	
S100P #2	Sense	CAC GUC UGC CUG UCA CAA GUA TT	
	Anti-sense	UAC UUG UGA CAG GCA GAC GUG TT	
Ezrin #1	Sense	GGA GCA GCA CCU UCA GGA UTT	MFM-223: 25 nM
	Anti-sense	AUC CUG AAG UGC UGC UCC TT	
Ezrin #2	Sense	AAG CAG CAG CUG AAC AAC AUG TT	SUM-185-PE: 30 nM
	Anti-sense	CAU GUU GUU CAG CUG CUG CUU TT	
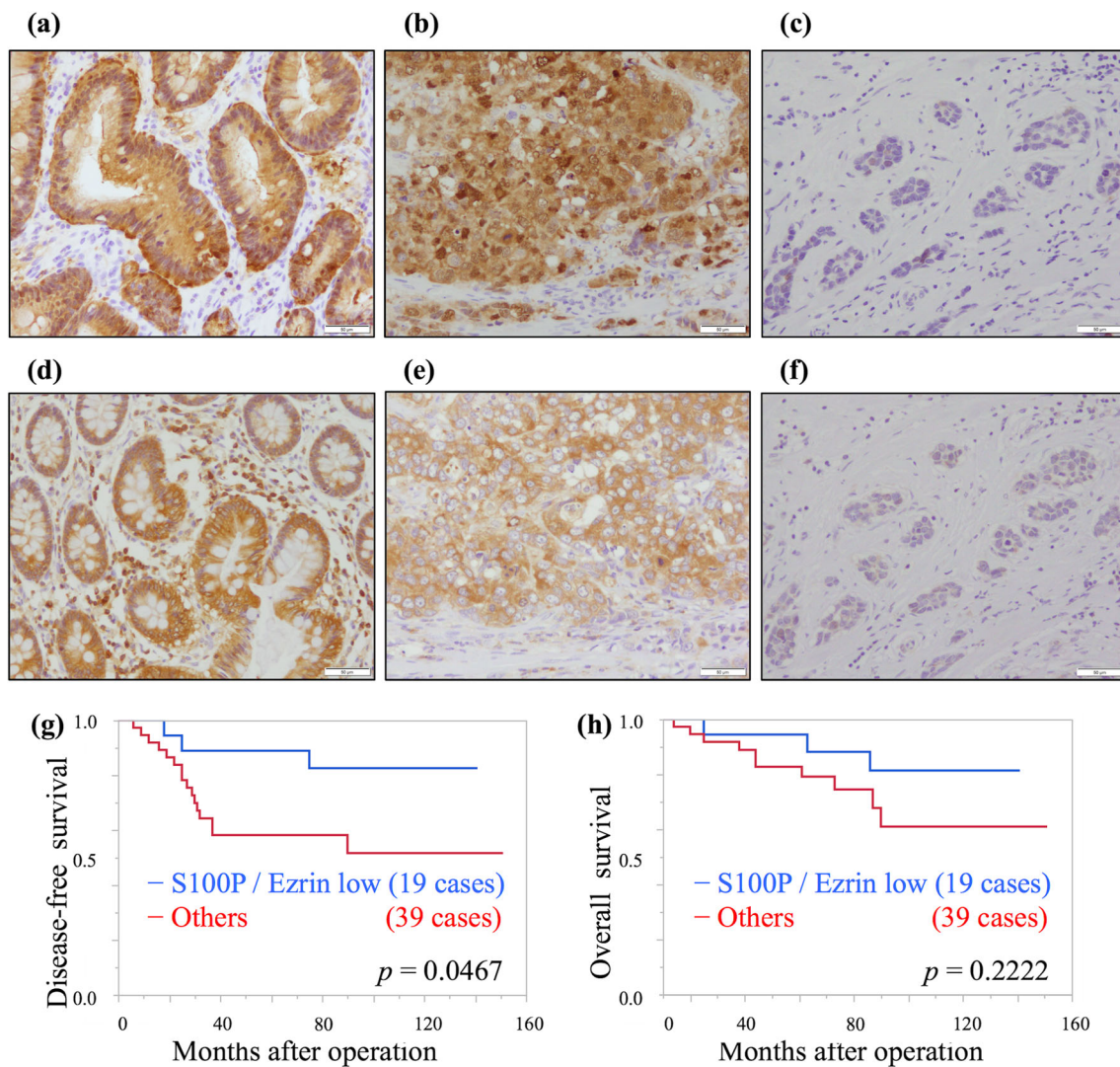
Fig. 1 S100P and Ezrin immunoreactivity is significantly associated with a worse disease-free survival of TNBC patients. (**a-c**) Representative illustrations of S100P expression in normal stomach (positive control; a) and S100P-positive (b) and -negative (c) TNBC cases. (**d-f**) Representative illustrations of Ezrin expression in normal colon (positive control; d) and Ezrin-positive (e) and -negative (f) TNBC cases. (**g**) Disease-free survival and (**h**) overall survival of TNBC patients according to their combined S100P and Ezrin expression status using Kaplan-Meier analyses. Statistical significance was assessed using the Wilcoxon test. Scale bar = 50 μm

tubes after which total RNA was precipitated using isopropanol (Wako). Following centrifugation (13,000 rpm, 4 °C, 10 min), RNA pellets were washed twice in 70% ethanol (Wako), allowed to dry and dissolved in distilled water (Qiagen). After measurement of the RNA concentrations using Nano Drop One equipment (Thermo Fisher Scientific), cDNA was synthesized using a QuantiTect reverse transcription kit (Qiagen, Hilden, Germany) according to the manufacturer's instructions. In brief, 1 μg RNA of each sample was incubated with gDNA Wipeout Buffer (2 μl) and RNase free water (variable, 14 μl of total reaction volume) for 2 min at 42 °C in a Life Touch Thermal Cycler (Bioer Technology, Hangzhou, China). After the subsequent addition of Quantiscript RT buffer (4 μl), a RT Primer Mix (1 μl) and Quantiscript Reverse Transcriptase (1 μl), cDNA was synthesized through incubation for 30 min at 42 °C and

3 min at 95 °C in a Thermal Cycler. qRT-PCR was carried out in triplicate using a LightCycler 96 System (Roche Diagnostics, Mannheim, Germany) in conjunction with a FastStart Essential DNA Green Master (Roche) according to the manufacture's instruction. Reactions were performed as follows: 15 min 95 °C → 10 s 95 °C, 10 s 63 °C, 15 s 72 °C (40 cycles). All mRNA quantitative data were normalized to the RPL13A expression level. Primers were obtained from Nihon Gene Laboratories (Miyagi, Japan) and their sequences are listed in Table 2.

2.5 Western blotting

Total cell protein samples were extracted using Mammalian Protein Reagent (M-PER, Thermo Fisher Scientific)

Table 4 Correlations between the S100P / Ezrin combination status and clinicopathological features in TNBC cases

		S100P / Ezrin ($n = 58$)		p value
		Double low ($n = 19$, 32.8%)	Others ($n = 39$, 67.2%)	
Age		52.1 ± 2.9	56.9 ± 2.0	0.1785
Tumor size	< 2 cm	7 (41.2%)	22 (59.5%)	
	≥ 2 cm	10 (58.8%)	15 (40.5%)	0.2105
Stage	1	5 (27.8%)	15 (41.7%)	
	2	9 (50.0%)	13 (36.1%)	
	3	4 (22.2%)	8 (22.2%)	0.5470
Histological grade	1	2 (11.1%)	0 (0.0%)	
	2	3 (16.7%)	8 (21.6%)	
	3	13 (72.2%)	29 (73.0%)	0.1965
LYV	−	13 (72.2%)	10 (27.0%)	
	+	10 (55.6%)	27 (73.0%)	0.1965
Lymph node metastasis	−	13 (72.2%)	23 (62.2%)	
	+	5 (27.8%)	14 (37.8%)	0.4572
Ki-67 LI		35.3 ± 6.8	49.1 ± 4.8	0.1045

Age and Ki-67 LI are presented as mean ± SEM. All other values represent numbers of cases and percentages

LYV, lymph and vascular invasion

containing 1% Halt Protease Inhibitor Cocktail (Pierce Biotechnology, Rockford, IL, USA) and EDTA (Pierce Biotechnology) followed by centrifugation for 10 min at 4 °C and 15,000 rpm. The protein concentrations were measured using a Protein Assay Rapid kit (Wako), based on a pyrogallol red method. Next, approximately 15 μg protein samples were denatured in a Sample Buffer Solution (Wako) supplemented with 2-mercaptoethanol (Wako) for 4 min at 100 °C, subjected to SDS-PAGE and transferred to Immobilon Transfer Membranes (Merck Millipore, Billerica, MA, USA). After blocking with TBS containing 0.05% Tween 20 (TBS-T, Wako) and 5% skim milk (Wako), the membranes were incubated overnight at 4 °C with primary antibodies (listed in Table 1). Subsequently, the membranes were washed with TBS-T and incubated with HRP-conjugated Mouse IgG (GE Healthcare, Buckinghamashire, UK) or HRP-conjugated Rabbit IgG (GE Healthcare) for 1 h at room temperature. Finally, the membranes were washed with TBS-T and the protein bands were visualized using an ECL-Prime Western Blotting Detection Reagent (GE Healthcare) in conjunction with a ChemiDoc XRS+ System (Bio-Rad, Hercules, CA, USA).

2.6 Small interfering RNA (siRNA) transfection

siRNA transfections were performed using a MISSION Universal Negative Control siRNA (siNC) and S100P and Ezrin MISSION siRNAs (Sigma-Aldrich). The target sequences of the siRNAs are listed in Table 3. Appropriate amounts of siRNA were incubated with Opti-MEM (Life

Technologies) and Lipofectamine RNAiMAX (Invitrogen, Carlsbad, CA, USA) for 30 min at room temperature, after which each siRNA was transfected into MFM-223 and SUM-185-PE cells for 72 h.

2.7 Cell proliferation assay

Cell cultures were performed at 37 °C in a 5% CO_2 incubator. Changes in cell proliferation were evaluated in quintuplicate using a Cell Counting Kit-8 assay (CCK-8; Dojindo, Kumamoto, Japan), based on a WST-8 [2- (2-methoxy-4-nitrophenyl)-3-(4-nitrophenyl)-5-(2,4-disulfophenyl)-2H-tetrazolium, monosodium salt] method according to the manufacturer's instructions.

2.8 Cell migration assay

Cell migration assays were performed using Cell Culture Insert Transparent PET membranes with 8.0 μm pores

Table 5 Subtypes of breast carcinoma cell lines used in this study

No.	1	2	3	4
Cell	MDA-MB-231	MDA-MB-453	MFM-223	SUM-185-PE
Subtype	TNBC	HER2	TNBC	TNBC
No.	5	6	7	8
Cell	MCF-7	T-47D	ZR-75-1	SK-BR-3
Subtype	Luminal A	Luminal A	Luminal A	HER2

inserted in 24-well plates (CORNING, NY, USA). siRNA transfected MFM-223 cells were seeded in the upper chambers in serum-free Minimum Essential Media (MEM), while MEM containing 10% FBS was added to the bottom chambers. After incubation for 24 h, the cells on the upper surface of the membranes were mechanically removed with cotton swabs. The migrated cells (lower surface) were fixed in methanol for 10 min and stained with hematoxylin for 30 min at room temperature. Next, the membranes were mounted on glass slides and the migration rates were evaluated as the average number of cells in nine randomly selected fields (each three fields in triplicate, ×200 under an optical microscope) on the membrane surfaces.
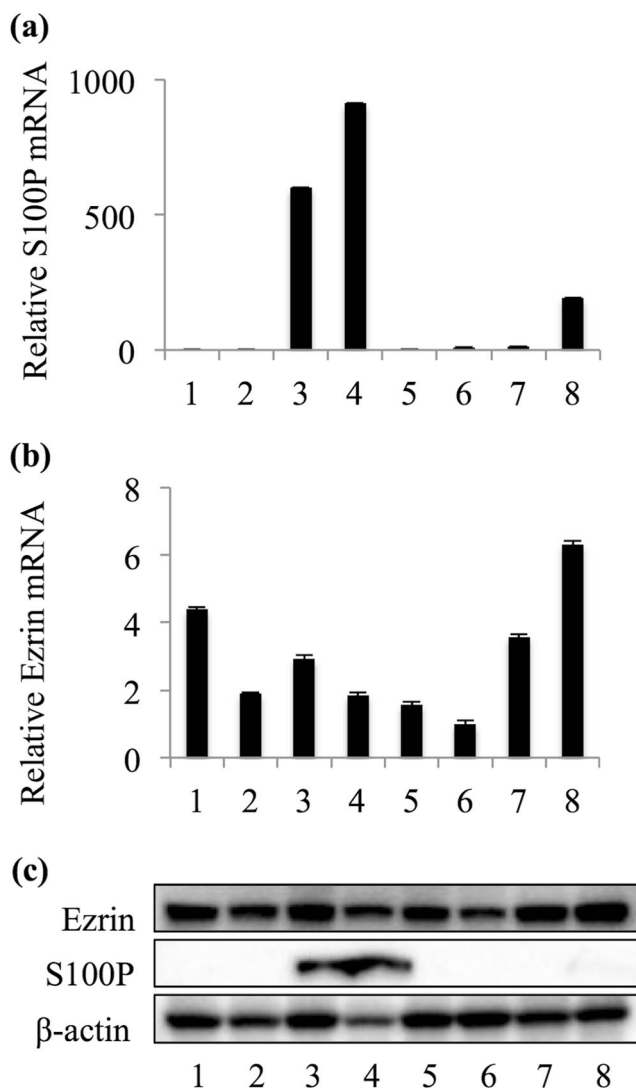
Fig. 2 S100P is overexpressed in TNBC-derived cell lines. mRNA expression levels of (a) S100P and (b) Ezrin in various breast cancer-derived cell lines determined by qRT-PCR. The data are presented as mean ± standard deviation. (c) S100P and Ezrin protein expression determined by Western blotting. 1: MDA-MB-231, 2: MDA-MB-453, 3: MFM-223, 4: SUM-185-PE, 5:MCF-7, 6: T-47D, 7: ZR-75-1 and 8: SK-BR-3 cells

## 2.9 Trans-endothelial migration assay

For the trans-endothelial migration (TEM) assays two time courses were used, i.e., a short term (1 min - 1 h) [32] and a long term (24 h) course [33]. The long term TEM assay was used to screen selected cell lines for their trans-endothelial migration ability. For this assay Millicell 8-well glass EZ slides were used (EMD Millipore, Billerica, MA, USA). 1.0×10^6 HUEhT-1 cells were seeded onto 8-well glass slides and allowed to grow for approximately 24 h to form monolayers. After washing with PBS, 8×10^4 carcinoma cells were added onto the monolayers and allowed to trans-endothelially migrate for 24 h. Following removal of the non-migrated carcinoma cells by washing with PBS, the migrated carcinoma cells and HUEhT-1 cells were fixed with 10% Formalin Neutral Buffer Solution (Wako) for 10 min at room temperature and, subsequently, permeabilized with 0.1% Triton X-100 (Sigma-Aldrich) for 15 min at room temperature. After blocking with 10% goat normal serum (Nichirei) for 30 min at room temperature, the cells on the slides were incubated overnight at 4 °C with a primary pan-Cytokeratin antibody as a marker of epithelial cells in order to quantify their migration. The conditions for the primary antibody are presented in Table 1. Next, the cells on the slides were incubated with EnVisionTM+ Dual Link System-HRP (DAKO, Carpinteria, CA, USA) for 1 h at room temperature and visualized using a 3, 3-diaminobenzidine (DAB) solution. Finally, the cells were counterstained with hematoxylin and trans-endothelial migration rates were evaluated as average values of positive areas in six randomly selected fields (each three fields in duplicate, ×100 under an optical microscope) using Lumina vision (Mitani Corporation, Fukuoka, Japan).

For the short term TEM assay a xCELLigence Real Time Analyzer DP (ACEA Biosciences, San Diego, CA, USA) was used. Through this system, electrical impedance across gold microelectrodes integrated in the bottom of cell culture plates are measured in real time in order to determine the cohesiveness of a cellular monolayer. Specifically, 50 μl culture medium was added to an E-Plate VIEW 16 plate (ACEA Biosciences) after which background electrical impedance was measured. Next, 1.0×10^4 HUEhT-1 cells were seeded into the plate after which monolayers were allowed to establish during approximately 28 h. Finally, 4×10^4 MFM-223 cells were added to the HUEhT-1 monolayers and the electrical impedances were measured during 1 h with 1 min intervals. All data in duplicate were normalized to the cell cohesiveness index at the time of addition of the MFM223 cells.

2.10 Statistical analysis

All statistical analyses were performed using JMP Pro 13.1.0 (SAS Institute, Tokyo, Japan). For immunohistochemistry, associations between IHC and clinicopathological features were

Fig. 3 S100P and Ezrin expression are downregulated after siRNA transfection. MFM-223 and SUM-185-PE, both TNBC cell lines, were transfected with a negative control siRNA and siRNAs directed against S100P or Ezrin for 72 h. The protein expression levels of S100P and Ezrin were determined by Western blotting
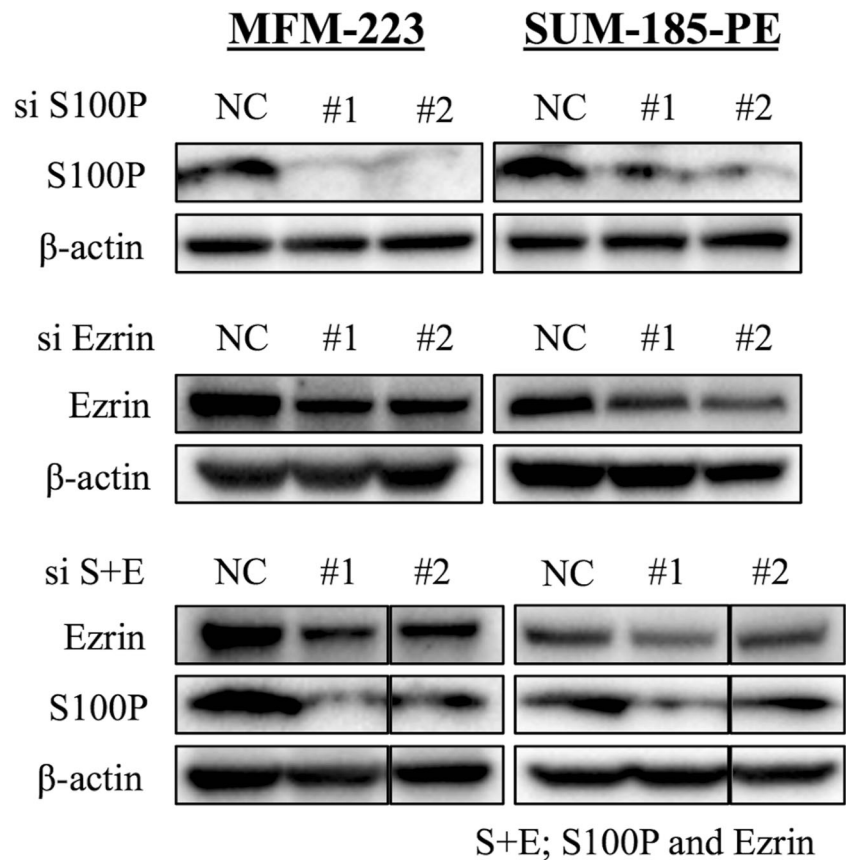
evaluated using ANOVA or Pearson's χ^2 tests. Disease-free survival (DFS) and overall survival (OS) rates were analyzed using the Kaplan-Meyer method, and assessed by Wilcoxon test. The results of the in vitro studies are presented as mean ± standard deviation, with significant differences between two groups evaluated by Dunnett's test and multiple comparisons by Tukey's test. A p value < 0.05 was considered to be statistically significant.
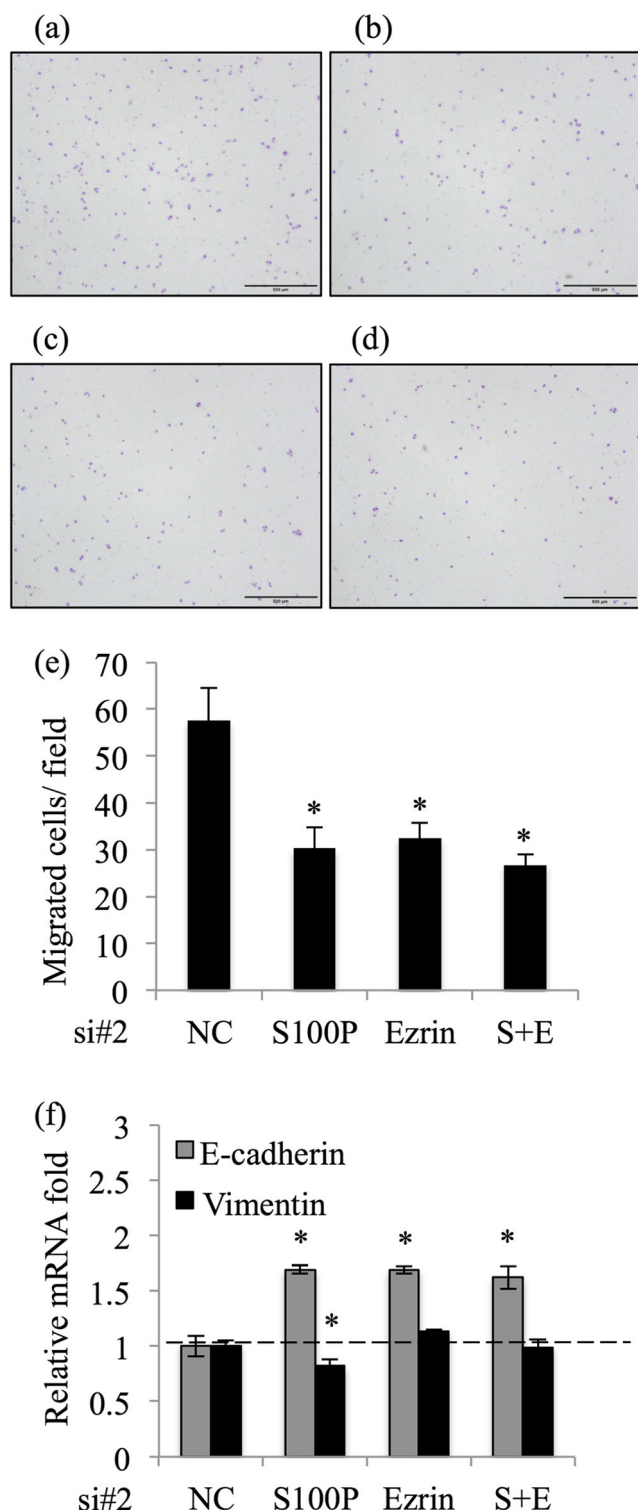
3 Results

3.1 Co-expression of S100P and Ezrin correlates with a worse DFS in TNBC patients

In order to investigate the possible relevance of S100P and Ezrin in TNBC, we first examined their expression in 58 primary tumor samples by immunohistochemistry (IHC). We found that S100P and Ezrin were mainly localized in the cytoplasm of the tumor cells (Fig. 1a-f). A relatively high S100P immunoreactivity was observed in 17 out of 58 (29.3%) cases, and was found to significantly correlate with the Ki-67 labeling index (LI) ($p = 0.0306$, Supplementary Table 1). Likewise, a relatively high Ezrin immunoreactivity was observed in 37 out of 58 (63.8%) cases, and trended towards a correlation with the Ki-67 LI ($p = 0.0833$, Supplementary Table 2).

Next, the cohort was classified into two groups, low: S100P and Ezrin double low cases, high: S100P or Ezrin single high cases and S100P and Ezrin double high cases. We found that the combined expression status of S100P and Ezrin was not associated with any of the clinicopathological features tested (Table 4). Upon survival analyses, we found that TNBC patients with a double low S100P and Ezrin expression had a better DFS compared to the other TNBC patients ($p = 0.0467$, Fig. 1g). On the other hand, we found that the OS of the TNBC patients was not significantly different according to their combined S100P and Ezrin expression status (Fig. 1h).

3.2 S100P and Ezrin are markedly expressed in TNBC-derived cell lines

In order to select appropriate cells for subsequent in vitro experiments, we set out to examine the expression of S100P and Ezrin in various breast cancer-derived cell lines (listed in Table 5) by qRT-PCR and Western blotting. We found that Ezrin was expressed in all cell lines tested at both the mRNA (Fig. 2b) and protein (Fig. 2c) levels, while S100P was found to be expressed in only two TNBC-derived cell lines, MFM-223 and SUM-185-PE, at the protein level (Fig. 2a, c). Therefore, the MFM-223 and SUM-185-PE cell lines were selected for our further experiments.

3.3 S100P and Ezrin induce proliferation and migration in TNBC-derived cells

According to the IHC data reported above, the S100P and Ezrin expression status trended towards a correlation with the Ki-67 LI in the TNBC patient samples. Therefore, we set out to examine the involvement of both S100P and Ezrin in the proliferation of TNBC-derived cells in vitro. To this end, MFM-223 and SUM-185-PE cells were transfected with S100P and Ezrin siRNAs, after which their proliferation was assessed using a CCK-8 assay (Fig. 3). We found that single knockdown of S100P and double knockdown of S100P and Ezrin significantly inhibited the proliferation of these two cell lines compared to that of control cells (Supplementary Fig. 1).

Based on our IHC analyses, S100P and Ezrin expression were found to be associated with metastatic recurrences (DFS) in TNBC patients. As migration is a cellular process closely related to metastasis, we next set out to elucidate putative effects of S100P and Ezrin expression on the migration of TNBC cells. To this end, a migration assay was performed with S100P and Ezrin siRNA-transfected MFM-223 cells. SUM-185-PE cells were not included in this assay as they did not show a sufficient basal level of migration. We found that all MFM-223 cells transfected with targeted siRNAs (Ezrin, S100P or both) exhibited a significantly reduced migration capacity compared to that of control cells (Fig. 4a-e). Based on these results, the expression of Epithelial-Mesenchymal Transition (EMT) markers was examined by qRT-PCR. We found that the expression of E-cadherin, an epithelial marker [34], was significantly upregulated in all MFM-223 cells transfected with a targeted siRNA compared to that of control cells (Fig. 4f). Conversely, we found that the expression of Vimentin, a mesenchymal marker [34], was

Fig. 4 S100P and Ezrin promote the migration of TNBC cells. (a-d) Representative illustrations of cells transfected with (a) negative control, (b) S100P, (c) Ezrin and (d) S100P and Ezrin siRNAs. Scale bar = 500 μm. (e) Migrated cells evaluated as the average number of cells in nine fields randomly selected on the lower surface of the membrane using optical microscopy. (f) Expression of E-cadherin and Vimentin as epithelial and mesenchymal markers, respectively, determined by qRT-PCR. The data are presented as mean ± standard deviation. S + E: S100P and Ezrin, *$p < 0.05$

Fig. 5 S100P and Ezrin attenuate intercellular junctions of endothelial ▶ cells and accelerate the trans-endothelial migration of MFM-223 cells. (a) Representative illustrations of trans-endothelial migration of MFM-223 cells visualized by pan-Cytokeratin immunocytochemistry (ICC). Scale bar = 200 μm. (b) Trans-endothelial migration of MFM-223 cells evaluated as the average of pan-Cytokeratin positive areas in six randomly selected fields using optical microscopy in conjunction with Lumina vision. S100P and Ezrin attenuate intercellular junctions of endothelial cells and accelerate trans-endothelial migration of SUM-185-PE cells. (c) Representative illustrations of trans-endothelial migration of SUM-185-PE cells by pan-Cytokeratin ICC. Scale bar = 100 μm. (d) Trans-endothelial migration of SUM-185-PE cells evaluated as the average of pan-Cytokeratin positive areas in six randomly selected fields using optical microscopy in conjunction with Lumina vision. The data are presented as mean ± standard deviation. S + E: S100P and Ezrin. *$p < 0.05$. (e) Impedance (cell index) measurement monitored in real time by xCELLigence. The normalized cell index of HUEhT-1, an immortalized human umbilical vein endothelial cell line, was calculated using RTCA software. In the horizontal axis the time of MFM-223 dissemination was set at zero. (f) Relative cell index at 1 h after MFM-223 dissemination calculated using RTCA software. The data are presented as mean ± standard deviation. 223: MFM-223, H: HUEhT-1, S: S100P, E: Ezrin, S + E: S100P and Ezrin. *$p < 0.05$

(a)

(b)

(c)

(d)

(e)

(d)
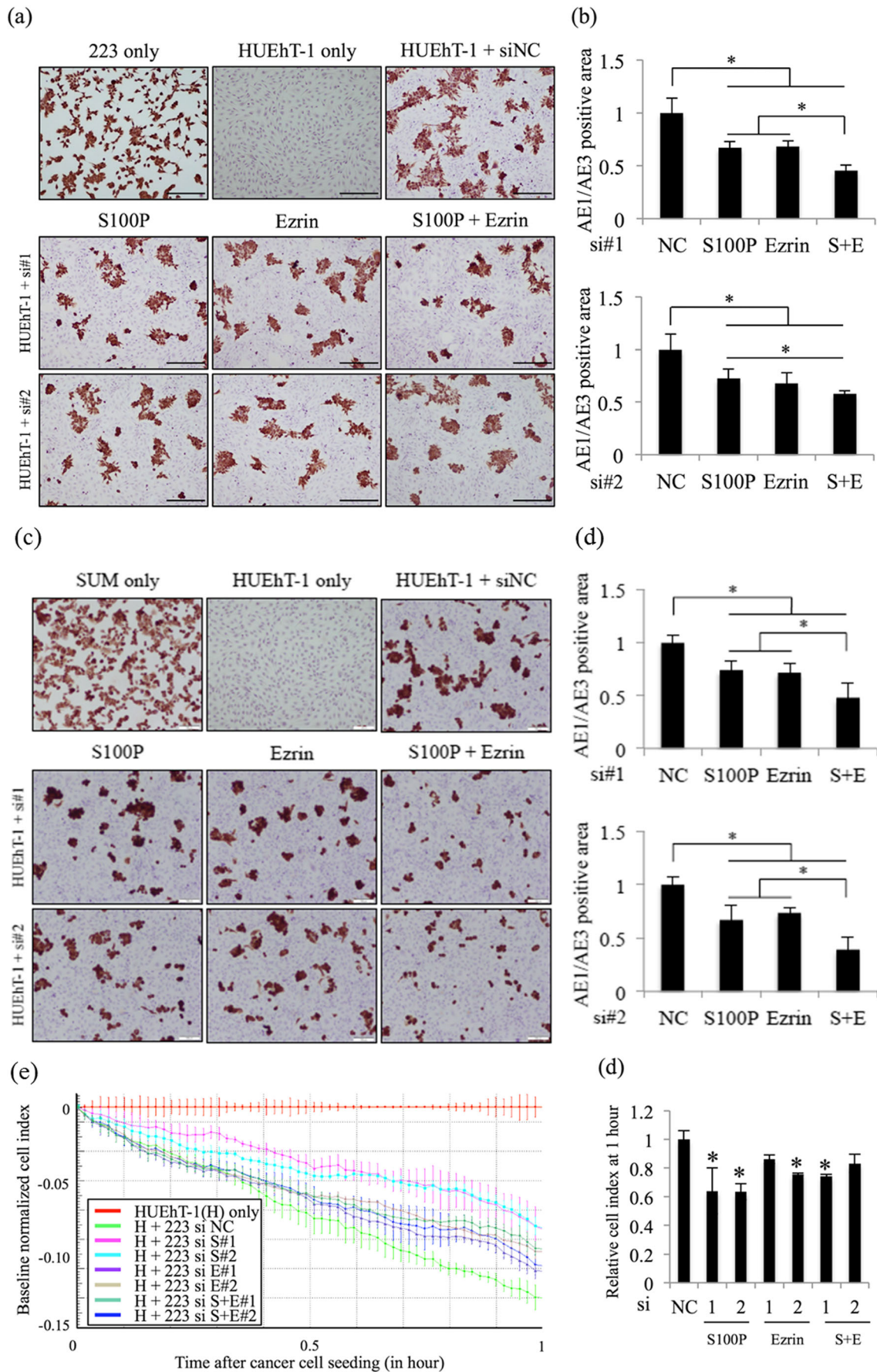
significantly inhibited only in MFM-223 transfected with a S100P siRNA compared to that of control cells (Fig. 4f).

## 3.4 S100P and Ezrin enhance trans-endothelial migration of TNBC-derived cells

To investigate the involvement of S100P and Ezrin in the trans-endothelial migration of TNBC cells, a long term (24 h) TEM assay was carried out using S100P and Ezrin siRNA transfected MFM-223 and SUM-185-PE cells. We found that a single siRNA-mediated knockdown of S100P or Ezrin significantly decreased the TEM of MFM-223 cells compared to that of control cells. In addition, we found that a double knockdown of S100P and Ezrin significantly decreased the TEM of MFM-223 cells compared to that of single 100P or Ezrin knockdown MFM-223 cells (Fig. 5a, b). Similar results were obtained with SUM-185-PE cells (Fig. 5c, d).

Short-term (up to 1 h) changes in TEM following S100P and/or Esrin knockdown were also examined by xCELLigence Real Time Analyzer DP. This approach has the technical advantages of removing the effects of proliferation and intercellular adhesion through short term measurement of cellular interactions, thus being able to confirm the validity of the results in the long term TEM assay used above. Due to limited access to this technology, the experiments were only performed on MFM-223 cells. These cells showed stronger results in the long term TEM assay and exhibited a more pronounced EMT phenotype in the qRT-PCR assays above. We did not observe significant differences in the TEM between single and double S100P and Ezrin knockdown MFM-223 cells, but found that S100P and Ezrin knockdown significantly decreased the rate at which the impedance of the HUEhT-1 monolayer was lowered compared to that of MFM-223 control cells, suggesting that even over a short time period S100P and Ezrin knockdown may abrogate TEM (Fig. 5e, f).

3.5 Ezrin$^{Thr-567}$ expression status is associated with TNBC lymph and vascular invasion

Although we found that S100P and Ezrin expression may be involved in the TEM of TNBC cells in vitro, an in vivo correlation with lymph and/or vascular invasion still remains to be established (Table 4). To this end, we decided to assess the expression of Ezrin$^{Thr-567}$, the phosphorylated, active form of the protein, in primary TNBC samples. We found that Ezrin$^{Thr-567}$ was localized in both the cytoplasm and the membranes of TNBC cells. Representative images are shown in Fig. 6a-c. A high immunoreactivity was observed in 27 out of 58 (46.6%) cases. In addition, we found that the Ezrin$^{Thr-567}$ expression status was significantly correlated with lymph and
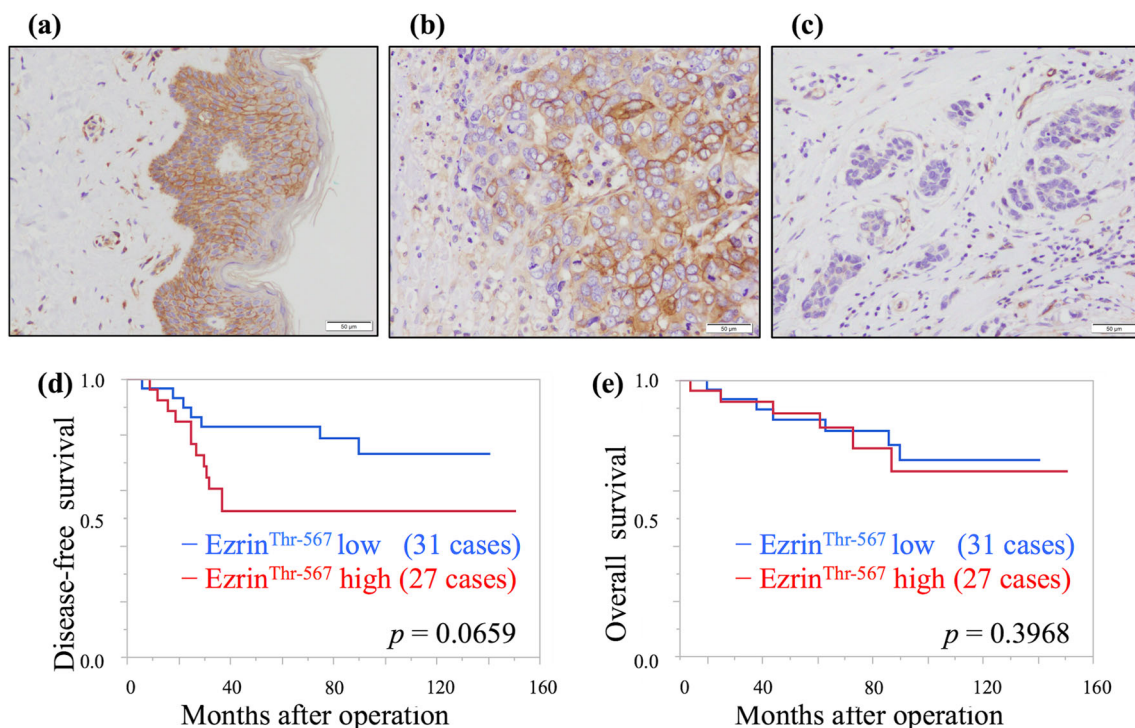
Fig. 6 Ezrin$^{Thr-567}$ immunoreactivity is significantly associated with lymph and vascular invasion in TNBC patients. (**a-c**) Representative illustrations of Ezrin$^{Thr-567}$ expression in normal skin (positive control; a) and Ezrin$^{Thr-567}$-positive (b) and -negative (c) TNBC cases. (**d**) Disease-free survival and (**e**) overall survival of TNBC patients according to Ezrin$^{Thr-567}$ expression status using Kaplan-Meier analyses. Statistical significance was analyzed using the Wilcoxon test. Scale bar = 50 μm

Table 6 Correlations between Ezrin$^{Thr-567}$ expression and clinicopathological features in TNBC cases

		Ezrin$^{Thr-567}$ (n = 58)		*p* value
		Low (*n* = 31, 53.4%)	High (*n* = 27, 46.6%)	
Age		55.4 ± 2.3	55.2 ± 2.5	0.9615
Tumor size	< 2 cm	15 (53.6%)	14 (53.9%)	
	≥ 2 cm	13 (46.4%)	12 (46.1%)	0.9839
Stage	1	10 (34.5%)	10 (40.0%)	
	2	13 (44.8%)	9 (36.0%)	
	3	6 (20.7%)	6 (24.0%)	0.8046
Histological grade	1	2 (6.9%)	0 (0.0%)	
	2	5 (17.2%)	6 (23.1%)	
	3	22 (75.9%)	20 (76.9%)	0.2472
LYV	–	13 (44.8%)	5 (19.2%)	
	+	16 (55.2%)	21 (80.8%)	*0.0405*
Lymph node metastasis	–	21 (72.4%)	15 (57.7%)	
	+	8 (27.6%)	11 (42.3%)	0.2512
Ki-67 LI		35.2 ± 5.2	55.3 ± 5.6	**0.0110**

Age and Ki-67 LI are presented as mean ± SEM. All other values represent numbers of cases and percentages. Significant correlations are shown in bold. LYV: lymph and vascular invasion

vascular invasion (*p* = 0.0405, Table 6) and the Ki-67 LI (*p* = 0.0110, Table 6). Upon survival analyses, we found that patients with a low of Ezrin$^{Thr-567}$ expression tended towards a better DFS compared to those with a high expression (*p* = 0.0659, Fig. 6d). No significant differences were noted with respect to OS (Fig. 6e).

4 Discussion

We investigated the expression of S100P and Ezrin in a cohort of TNBC patients and its correlation with clinicopathological features. We found that a combined expression of S100P and Ezrin was significantly correlated with a worse DFS, and that the (activated) Ezrin$^{Thr-567}$ status was significantly associated with lymph and vascular invasion in TNBC patients. In addition, we found that a combined expression of S100P and Ezrin promoted the migration and trans-endothelial migration (TEM) of TNBC-derived cells. This is the first study showing the involvement of S100P, Ezrin and Ezrin$^{Thr-567}$ in the TEM of TNBC, both in vitro and in vivo.

Previously, it has been reported that membranous Ezrin expression in breast cancer may be negatively correlated with the Ki-67 LI, whereas cytoplasmic Ezrin expression may be positively correlated with the Ki-67 LI [35]. These data suggest that the role of Ezrin in regulating breast cancer cell proliferation may differ, depending on its intracellular sub-localization. As the majority of Ezrin immunoreactivity observed in our cohort was cytoplasmic in nature, the results reported by Sarrio et al. [35] appear to be in agreement with ours, in that the Ezrin positive cases exhibited a higher proliferation rate and, hence,

a worse prognosis. Another previous in vitro study, aimed at uncovering the effect of knocking down Ezrin in the MDA-MB-231 TNBC cell line, revealed only a minor effect on its proliferation rate [25]. Conversely, we found that Ezrin knockdown in TNBC cell lines expressing both S100P and Ezrin resulted in significantly reduced proliferation rates.

Likewise, it has previously been reported that S100P expression may be correlated with the Ki-67 LI in primary breast cancer lesions [36], which would agree with our findings in the current TNBC cohort. Next to studies showing a direct effect of S100P expression on breast cancer cell proliferation, a myriad of studies has suggested its association with a proliferative state across a number of cancers, including endometrium and colon cancer [37–46], suggesting a common phenomenon across cancer types. Mechanistically, S100P has previously been shown to promote cellular proliferation through binding to RAGE (Receptor for Advanced Glycation End Products) and activation of downstream factors such as ERKs (Extracellular-regulated kinases), NF-κB (Nuclear factor-kappa B) [44, 47] and β-catenin [37]. The latter factors are particularly interesting as they have already been shown to act as important players in aggressive breast cancer behavior, suggesting that S100P may be embedded in a wider network of known breast cancer drivers.

While the clinical data from our present study do not allow verification of a direct interaction between S100P and Ezrin in TNBC, previous studies have reported that such interactions in other cancer cells may have an effect on their metastatic behavior [26, 30]. In hepatocellular carcinoma, Ezrin has been found to be phosphorylated at Thr-567 by Rho kinase and to subsequently promote the metastasis of these carcinoma cells [48], suggesting an involvement of Rho in the phosphorylation and

activation of Ezrin. Giampieri et al. [49] found that Rho kinase-associated signaling pathways may be involved in the promotion of migration and metastasis of breast cancer cells. Thus, despite the fact that we did not show a direct interaction between Ezrin and S100P, we considered it important to assess these proteins not only in isolation, but also in combination.

Since Ezrin and S100P in combination or in isolation have been suggested to play a role in either physical or endothelial cell migration in various cancers, including lung [29, 30, 50], breast (luminal and subtype not specified) [25, 46], gastric [51], colon [52] and pancreatic cancer [31, 53], we set out to explore their effect in two suitable TNBC-derived cell lines. We found that siRNA-mediated knockdown of either or both Ezrin and S100P reduced the migratory ability of these cell lines concomitant with an increased E-Cadherin expression, confirming an important role of both proteins in migration and establishing the EMT phenotype. Mechanistically, it has previously been found that S100P may induce EMT through binding to Integrin $\alpha 7$ and subsequent activation of the FAK (Focal Adhesion Kinase)/Src/Akt pathway, and enhancement of the expression of ZEB1, which is a known EMT marker [50]. Ezrin has also been reported to promote EMT through NF-κB activation [52]. Since many of these pathways are known to play roles in breast cancer progression, it adds credence to the idea that also Ezrin and S100P may act as central players, but further studies are required to elucidate the exact mechanistic underpinnings of this process.

In summary, we found that S100P and Ezrin may promote the trans-endothelial migration of TNBC cells. Both S100P and Ezrin, and the phosphorylated form Ezrin$^{Thr-567}$, were found to be involved in the proliferation and recurrence of TNBC. While we acknowledge that the cohort used in this study is relatively small and that ideally these findings should be replicated in a larger series, the indication that these two proteins may regulate fundamental processes leading to adverse clinical outcomes is an important one. A further elucidation of the precise mechanisms underlying the trans-endothelial migration of breast cancer cells may contribute to development of novel treatment strategies, not only for TNBC patients, but also for patients suffering from various other malignancies.

Compliance with ethical standards

This study was approved by Ethics Committee at Tohoku University School of Medicine. Informed consent was obtained from all patients.

Conflict of interest The authors declare that they have no conflict of interest.

References

1. K.R. Bauer, M. Brown, R.D. Cress, C.A. Parise, V. Caggiano, Descriptive analysis of estrogen receptor (ER)- negative, progesterone receptor (PR)-negative, and HER2-negative invasive breast cancer, the so-called triple-negative phenotype. Cancer **109**, 1721–1728 (2007)

2. M.D. Laurentiis, D. Cianniello, R. Caputo, B. Stanzione, G. Arpino, S. Cinieri, V. Lorusso, S.D. Placido, Treatment of triple negative breast cancer (TNBC): Current options and future perspectives. Cancer Treat Rev **36**, S80–S86 (2010)

3. R. Rouzier, C.M. Perou, W.F. Symmans, N. Ibrahim, M. Cristofanilli, K. Anderson, K.R. Hess, J. Stec, M. Ayers, P. Wagner, P. Morandi, C. Fan, I. Rabiul, J.S. Ross, G.N. Hortobagyi, L. Pusztai, Breast cancer molecular subtypes respond differently to preoperative chemotherapy. Clin Cancer Res **11**, 5678–5685 (2005)

4. C. Liedtke, C. Mazouni, K.R. Hess, F. Andre, A. Tordai, J.A. Mejia, W.F. Symmans, A.M. Gonzalez-Angulo, B. Hennessy, M. Green, M. Cristofanilli, G.N. Hortobagyi, L. Pusztai, Response to neoadjuvant therapy and long-term survival in patients with triple-negative breast cancer. J Clin Oncol **26**, 1275–1281 (2008)

5. R. Dent, M. Trudeau, K.I. Pritchard, W.M. Hanna, H.K. Kahn, C.A. Sawka, L.A. Lickley, E. Rawlinson, P. Sun, S.A. Narod, Triple-negative breast cancer; clinical features and patterns of recurrence. Clin Cancer Res **13**, 4429–4435 (2007)

6. M. Yousefi, R. Nosrati, A. Salmaninejad, S. Dehghani, A. Shahryari, A. Saberi, Organ-specific metastasis of breast cancer: Molecular and cellular mechanisms underlying lung metastasis. Cell Oncol **41**, 123–140 (2018)

7. R. Sharma, R. Sharma, T.P. Khaket, C. Dutta, B. Chakraborty, T.K. Mukherjee, Breast cancer metastasis: Putative therapeutic role of vascular cell adhesion molecule-1. Cell Oncol **40**, 199–208 (2017)

8. T. Arumugam, C.D. Logsdon, S100P: A novel therapeutic target for cancer. Amino Acids **41**, 893–899 (2011)

9. F. Prica, T. Radon, Y. Cheng, T. Crnogorac-Jurcevic, The life and works of S100P - from conception to cancer. Am J Cancer Res **6**, 562–576 (2016)

10. A. Maciejczyk, A. Łacko, M. Ekiert, E. Jagoda, T. Wysocka, R. Matkowski, A. Hałoń, B. Győrffy, H. Lage, P. Surowiak, Elevated nuclear S100P expression is associated with poor survival in early breast cancer patients. Histol Histopathol **28**, 513–524 (2013)

11. L. Chung, L. Phillips, M.Z. Lin, K. Moore, D.J. Marsh, F.M. Boyle, R.C. Baxter, A novel truncated form of S100P predicts disease-free survival in patients with lymph node positive breast cancer. Cancer Lett **368**, 64–70 (2015)

12. S. Zhang, Z. Wang, W. Liu, R. Lei, J. Shan, L. Li, X. Wang, Distinct prognostic values of S100 mRNA expression in breast cancer. Sci Rep **7**, 39786 (2017)

13. T. Becker, V. Gerke, E. Kube, K. Weber, S100P, a novel Ca^{2+}-binding protein from human placenta. cDNA cloning, recombinant protein expression and Ca^{2+} binding properties. Eur J Biochem **207**, 541–547 (1992)

14. S. Parkkila, P. Pan, A. Ward, A. Gibadulinova, I. Oveckova, S. Pastorekova, J. Pastorek, A.R. Martinez, H.O. Helin, J. Isola, The calcium-binding protein S100P in normal and malignant human tissues. BMC Clin Pathol **8**, 2 (2008)

15. M. Komatsu, T. Yoshimura, T. Matsuo, K. Kiyotani, Y. Miyoshi, T. Tanihashi, K. Rokutani, R. Yamaguchi, A. Saito, S. Imoto, S. Miyano, Y. Nakamura, M. Sasa, M. Shimada, T. Katagiri, Molecular features of triple negative breast cancer cells by genome-wide gene expression profiling analysis. Int J Oncol **42**, 478–506 (2013)

16. M. Maierthaler, M. Kriegsmann, C. Peng, S. Jauch, A. Szabo, M. Wallwiener, J. Rom, C. Sohn, A. Schneeweiss, H. Sinn, R. Yang, B.

Burwinkel, S100P and HYAL2 as prognostic markers for patients with triple-negative breast cancer. Exp Mol Pathol **99**, 180–187 (2015)

17. Q. Li, M. Wu, H. Wang, G. Xu, T. Zhu, Y. Zhang, P. Liu, A. Song, C. Gang, Z. Han, J. Zhou, L. Meng, Y. Lu, S. Wang, D. Ma, Ezrin silencing by small hairpin RNA reverses metastatic behaviors of human breast cancer cells. Cancer Lett **261**, 55–63 (2008)

18. S.D. Choi, Ezrin is an essential marker for metastasis of gynecologic cancer. J Korean Soc Menopause **18**, 81–93 (2012)

19. J. Clucas, F. Valderrama, ERM proteins in cancer progression. J Cell Sci **127**, 267–275 (2014)

20. T. Matsui, M. Maeda, Y. Doi, S. Yonemura, M. Amano, K. Kaibuchi, S. Tsukita, S. Tsukita, Rho-kinase phosphorylates COOH-terminal threonines of Ezrin/Radixin/Moesin (ERM) proteins and regulates their head-to-tail association. J Cell Biol **140**, 647–657 (1998)

21. A. Gautreau, D. Louvard, M. Arpin, Morphogenic effects of Ezrin require a phosphorylation-induced transition from oligomers to monomers at the plasma membrane. J Cell Biol **150**, 193–203 (2000)

22. J. Li, K. Wei, H. Yu, D. Jin, G. Wang, B. Yu, Prognostic value of Ezrin in various cancers: A systematic review and updated meta-analysis. Sci Rep **5**, 17903 (2015)

23. M. Bartova, J. Hlavaty, Y. Tan, C. Singer, K. Pohlodek, J. Luha, I. Walter, Expression of Ezrin and Moesin in primary breast carcinoma and matched lymph node metastases. Clin Exp Metastasis. **34**, 333–344 (2017)

24. T. Jin, J. Jin, X. Li, S. Zhang, Y.H. Choi, Y. Piao, X. Shen, Z. Lin, Prognostic implications of Ezrin and phosphorylated Ezrin expression in non-small cell lung cancer. BMC Cancer **14**, 191 (2014)

25. J. He, G. Ma, J. Qian, Y. Zhu, M. Liang, N. Yao, Q. Ding, L. Chen, X. Liu, T. Xia, S. Wang, Interaction between Ezrin and Cortactin in promoting epithelial to mesenchymal transition in breast cancer cells. Med Sci Monit **23**, 1583–1596 (2017)

26. M. Koltzscher, C. Neumann, S. Konig, V. Gerke, Ca²⁺-dependent binding and activation of dormant Ezrin by dimeric S100P. Mol Biol Cell **14**, 2372–2384 (2003)

27. H. Zhang, G. Wang, Y. Ding, Z. Wang, R. Barraclough, P.S. Rudland, D.G. Fernig, Z. Rao, The crystal structure at 2A resolution of the Ca²⁺-binding protein S100P. J Mol Biol **325**, 785–794 (2003)

28. A. Gibadulinova, V. Tothova, J. Pastorek, S. Pastorekova, Transcriptional regulation and functional implication of S100P in cancer. Amino Acids **41**, 885–892 (2011)

29. S. Diederichs, E. Bulk, B. Steffen, P. Ji, L. Tickenbrock, K. Lang, K.S. Zanker, R. Metzger, P.M. Schneider, V. Gerke, M. Thomas, W.E. Berdel, H. Serve, C. Muller-Tidow, S100 family members and trypsinogens are predictors of distant metastasis and survival in early-stage non-small cell lung cancer. Cancer Res **64**, 5564–5569 (2004)

30. J. Austermann, A.R. Nazmi, C. Muller-Tidow, V. Gerke, Characterization of the Ca²⁺-regulated Ezrin-S100P interaction and its role in tumor cell migration. J Biochem **283**, 29331–29340 (2008)

31. S. Barry, C. Chelala, K. Lines, M. Sunamura, A. Wang, F.M. Marelli-Berg, C. Brennan, N.R. Lemoine, T. Crnogorac-Jurcevic, S100P is a metastasis-associated gene that facilitates transendothelial migration of pancreatic cancer cells. Clin Exp Metastasis **30**, 251–264 (2013)

32. C. Artus, F. Glacial, K. Ganeshamoorthy, N. Ziegler, M. Godet, T. Guilbert, S. Liebner, P. Couraud, The Wnt/planar cell polarity signaling pathway contributes to the integrity of tight junctions in brain endothelial cells. J Cerebr Blood F Met **34**, 433–440 (2014)

33. N. Maishi, Y. Ohba, K. Akiyama, N. Ohga, J. Hamada, H. Nagao-Kitamoto, M.T. Alam, K. Yamamoto, T. Kawamoto, N. Inoue, A. Taketomi, M. Shindoh, Y. Hida, K. Hida, Tumour endothelial cells

in high metastatic tumours promote metastasis via epigenetic dysregulation of biglycan. Sci Reports **6**, 28039 (2016)

34. J.M. Iglesias, I. Beloqui, F. Garcia-Garcia, O. Leis, A. Vazquez-Martin, A. Eguiara, S. Cufi, A. Pavon, J.A. Menendez, J. Dopazo, A.G. Martin, Mammosphere formation in breast carcinoma cell lines depends upon expression of E-cadherin. PLoS One **e77281**, 8 (2013)

35. D. Sarrio, S.M. Maria, A. Dotor, F. Calero, D. Hardisson, J. Palacios, Abnormal ezrin localization is associated with clinico-pathological features in invasive breast carcinomas. Breast cancer Res Tr **98**, 71–79 (2006)

36. A.P.T. Schor, F.M. Carvalho, C. Kemp, I.D.C.G. Silva, J. Russo, S100P calcium-binding protein expression is associated with high-risk proliferative lesions of the breast. Oncol Rep **15**, 3–6 (2006)

37. L. Guo, S. Chen, H. Jiang, J. Huang, W. Jin, S. Yao, The expression of S100P increases and promotes cellular proliferation by increasing nuclear translocation of β-catenin in endometrial cancer. Int J Clin Exp Pathol **7**, 2102–2112 (2014)

38. Y. Liu, C. Wang, X. Shan, J. Wu, H. Liu, H. Liu, J. Zhang, W. Xu, Z. Sha, J. He, J. Fan, S100P is associated with proliferation and migration in nasopharyngeal carcinoma. Oncology Lett **14**, 525–532 (2017)

39. S. Dakhel, L. Padilla, J. Adan, M. Masa, J.M. Martinez, L. Roque, T. Coll, R. Hervas, C. Calvis, R. Messeguer, F. Mitjans, J.L. Hernandez, S100P antibody-mediated therapy as a new promising strategy for the treatment of pancreatic cancer. Oncogene **3**, e92 (2014)

40. J.K. Kim, K.H. Jung, J.H. Noh, J.W. Eun, H.J. Bae, H.J. Xie, Y.M. Ahn, J.C. Ryu, W.S. Park, J.Y. Lee, S.W. Nam, Targeted disruption of S100P suppresses tumor cell growth by down-regulation of cyclin D1 and CDK2 in human hepatocellular carcinoma. Int J Oncol **35**, 1257–1264 (2009)

41. X. Wang, T. Tian, M. Zhao, Y. Lou, J. Qian, Z. Liu, H. Chen, Z. Cui, High expression of S100P is associated with unfavorable prognosis and tumor progression in patients with epithelial ovarian cancer. Am J Cancer Res **5**, 2409–2421 (2015)

42. G.D. Basu, D.O. Azorsa, J.A. Kiefer, A.M. Rojas, S. Tuzmen, M.T. Barrett, J.M. Trent, O. Kallioniemi, S. Mousses, Functional evidence implicating S100P in prostate cancer progression. Int J Cancer **123**, 330–339 (2008)

43. A. Chandramouli, M.E. Mercado-Pimentel, A. Hutchinson, A. Gibadulinová, E.R. Olson, S. Dickinson, R. Shañas, J. Davenport, J. Owens, A.K. Bhattacharyya, J.W. Regan, S. Pastorekova, T. Arumugam, C.D. Logsdon, M.A. Nelson, The induction of S100p expression by the Prostaglandin E₂ (PGE₂)/EP4 receptor signaling pathway in colon cancer cells. Cancer Biol Ther **10**, 1056–1066 (2010)

44. M.E. Mercado-Pimentel, B.C. Onyeagucha, Q. Li, A.C. Pimentel, J. Jandova, M.A. Nelson, The S100P/RAGE signaling pathway regulates expression of microRNA-21 in colon cancer cells. FEBS Lett **589**, 2388–2393 (2015)

45. Z. Wu, T. Boonmars, I. Nagano, S. Boonjaraspinyo, P. Srinontong, P. Ratasuwan, K. Narong, P.S. Nielsen, Y. Maekawa, Significance of S100P as a biomarker in diagnosis, prognosis and therapy of opisthorchiasis-associated cholangiocarcinoma. Int J Cancer **138**, 396–408 (2015)

46. C. Zhou, Q. Zhong, L.V. Rhodes, I. Townley, M.R. Bratton, Q. Zhang, E.C. Martin, S. Elliott, B.M. Collins-Burow, M.E. Burow, G. Wang, Proteomic analysis of acquired tamoxifen resistance in MCF-7 cells reveals expression signatures associated with enhanced migration. Breast Cancer Res **14**, R45 (2012)

47. T. Arumugam, D.M. Simeone, A.M. Schmidt, C.D. Logsdon, S100P stimulates cell proliferation and survival via receptor for activated glycation end products (RAGE). J Biol Chem **279**, 5059–5065 (2004)

48. Y. Chen, D. Wang, Z. Guo, J. Zhao, B. Wu, H. Deng, T. Zhou, H. Xiang, F. Gao, X. Yu, J. Liao, T. Ward, P. Xia, C. Emenari, X. Ding, W. Thompson, K. Ma, J. Zhu, F. Aikhionbare, K. Dou, S.Y. Cheng, X. Yao, Rho kinase phosphorylation promotes Ezrin-mediated metastasis in hepatocellular carcinoma. Cancer Res **71**, 1721–1730 (2011)

49. S. Giampieri, C. Manning, S. Hooper, L. Jones, C.S. Hill, E. Sahai, Localized and reversible TGFβ signalling switches breast cancer cells from cohesive to single cell motility. Nat Cell Biol **11**, 1287–1296 (2009)

50. Y.L. Hsu, J.Y. Hung, Y.Y. Liang, Y.S. Lin, M.J. Tsai, S.H. Chou, C.Y. Lu, P.L. Kuo, S100P interacts with integrin α7 and increases cancer cell migration and invasion in lung cancer. Oncotarget **6**, 29585–29598 (2015)

51. L.L. Cao, J.W. Xie, Y. Lin, C.H. Zheng, P. Li, J.B. Wang, J.X. Lin, J. Lu, Q.Y. Chen, C.M. Huang, miR-183 inhibits invasion of gastric cancer by targeting Ezrin. Int J Clin Exp Pathol **7**, 5582–5594 (2014)

52. Y. Li, Z. Lin, B. Chen, S. Chen, Z. Jiang, T. Zhou, Z. Hou, Y. Wang, Ezrin/NF-kB activation regulates epithelial- mesenchymal transition induced by EGF and promotes metastasis of colorectal cancer. Biomed Pharmacother **92**, 140–148 (2017)

53. S. Hamada, K. Satoh, M. Hirota, W. Fujibuchi, A. Kanno, J. Umino, H. Ito, A. Satoh, K. Kikuta, K. Kume, A. Masamune, T. Shimosegawa, Expression of the calcium-binding protein S100P is regulated by bone morphogenetic protein in pancreatic duct epithelial cell lines. Cancer Sci **100**, 103–110 (2008)